

Supporting Information

Aromatic ring substituted g-C₃N₄ for enhanced photocatalytic hydrogen evolution

Yu Yu,^a Wei Yan,^a Wenyu Gao,^a Pei Li,^a Xiaofang Wang,^a Songmei Wu,^a Weiguo Song,^{*b} and Kejian Ding^{*b}

[†] School of Science, Beijing Jiaotong University, 100044 Beijing, PR China

[‡] Institute of Chemistry, Chinese Academy of Sciences, 100190 Beijing, PR China

Experimental

Synthesis of *BD-C₃N₄*: All of the chemicals were directly used without further purification, and the water used through the entire process was from MilliQ system. A designed dosage (i.e. 25 mg) of *m*-Trihydroxybenzene was mixed uniformly with 10 g urea in the state of solid, and then the mixture was transferred into a 30 cm × 60 cm rectangle crucible, which was covered by another identical crucible. The covered crucible was annealed for 1 h at 550 °C with the heating rate of 10 °C min⁻¹ in a muffle furnace, followed by a heat etching also for 1.5 h at the same temperature under the same heating rate excepted that the covering crucible was moved away. No pumping and purging the system with any inert gases was needed during the preparation. After the cooling of the polymerized product to room temperature, they were directly used for all the characterizations and measurements without any washing and purification. For the preparation of control sample as pure g-C₃N₄, all the procedure was the same except that no *m*-Trihydroxybenzene was added. As for other control samples, different amount of *m*-Trihydroxybenzene, or heating temperature and time were adopted when maintaining other parameters.

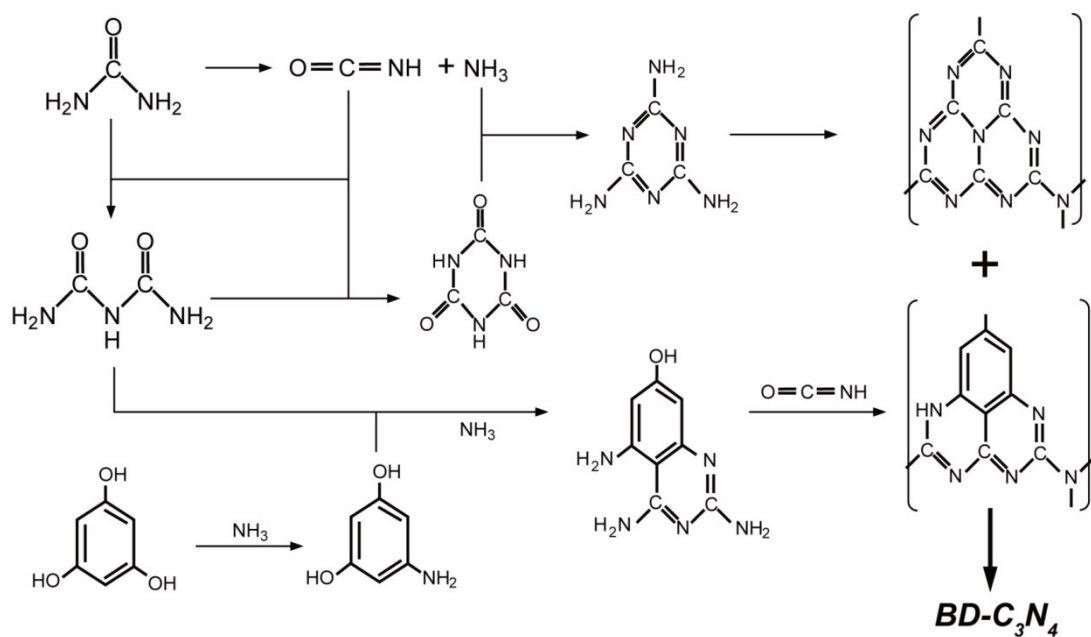
Characterization: SEM images accompanied with EDS results and TEM images were taken by scanning electron microscopy (SEM Hitachi-S4800) and transmission electron microscopy (TEM JEOL-2100F), respectively. Elements distribution mapping was also carried on SEM. X-Ray diffraction (XRD) patterns were recorded on a Rigaku diffractometer (Maxima XRD-7000) using Cu K α irradiation. XPS information was obtained on an ESCALAB250XI photoelectron spectroscopy. The proportion of all the elements was acquired by the elemental analyzer Thermo Flash EA 1112 elemental analyzer. IR and UV-visible absorption spectra were respectively obtained on Nicolet iN10 MX FT-IR Microscope and Shimadzu UV-2550 spectrophotometer with BaSO₄ as a reflectance standard. The specific surface area was measured by BET method on a JW-BK132F high performance micropore analyzer. Static and time-resolved decay fluorescence spectra were gathered on FLS980 fluorescence spectrometers ($\lambda_{\text{ext}} = 370$ nm). Atomic force microscope (AFM) images and height profiles were acquired through a Nanosurf Flex-Axiom microscope.

Theoretical calculation: The calculations were carried out based on density functional theory (hybrid functional, HSE06) using the Vienna ab-initio simulation package (VASP).¹ The generalized gradient approximation (GGA) using the Perdew-Burke-Ernzerhof (PBE) exchange correlation functional was employed, with the cut-off energy of 500 eV, total energy convergence of 1×10^{-4} eV and force convergence of 0.01 eV Å⁻¹. In the formation energy comparison, two different supercells ($4 \times 3 \times 1$ of eleven triazines + one benzene, Fig. S4c; $3 \times 2 \times 1$ of five pure tri-s-triazines + one benzene-containing tri-s-triazine, Fig. S4d) were adopted, while all other calculations were conducted in the latter configuration. The elementary composition of the two supercells were both 39 C : 45 N : 3 H, which was closed to that of the real sample by elemental analyzer. Only 2s and 2p states were considered for both C and N, respectively with 4 and 5 valence electrons. The Monkhorst–Pack scheme K points grid sampling was set as $5 \times 5 \times 3$ for the irreducible Brillouin zone. The band structures were calculated along the paths connecting the following high symmetry points: $\Gamma(0,0,0)$, A(0.5,0,0), H(0.5,0,0.5), K(0,0,0.5), $\Gamma(0,0,0)$, M(0,0.5,0), L(0,0.5,0.5), K(0,0,0.5) in the k-space.

Photocatalytic hydrogen evolution activity test: The photocatalytic reactions were carried out in PerfectLight Labsolar-III AI automatic online photocatalytic analysis system (Beijing Perfectlight Technology Co., Ltd.). 50 mg photocatalyst was well dispersed in a 100 mL aqueous solution containing triethanolamine (10 vol %) as sacrificial electron donors. In the case of deposition of Pt, an appropriate amount of H₂PtCl₆ aqueous solution was added into the photoreactor vessel. The reactant solution and the system were thoroughly evacuated several times to insure the complete removal of the air. The photocatalytic reaction was triggered by the visible-light irradiation offered by a 300 W Xe lamp (PLS-SXE

300, Beijing Trusttech Co. Ltd, China) with a 420 nm cut-off filter under continuous stirring. The temperature of the reactant solution was maintained under 12 °C by a flow of cooling water during the reaction. The amount of evolved H₂ was analyzed by an online gas chromatography (Fuli GC9790SD, TCD detector). For the cases of Pt deposition, the analysis was launched after the first half-hour Pt deposition and another evacuation of the system. The quantum efficiency (Φ) was estimated by the method described previously using the equation: $\Phi (\%) = (2 \times H/I) \times 100$, where H and I represent the numbers of evolved H₂ molecules and incident photons, respectively. For simplicity, it is assumed that all incident photons are absorbed by the photocatalyst.

Photoelectrochemical measurements: Photoelectrochemical measurements were performed with a CHI760 electrochemical workstation (CH Instruments, Inc., Shanghai) in 1 M Na₂SO₄ solution. In the standard three-electrode system, a Pt net and Ag/AgCl (saturated KCl) were used as the counter electrode and reference electrode, respectively. A L-shape glass carbon electrode (GCE) with the diameter of 4 mm was used as the working electrode. 10 mg photocatalyst was mixed with a certain amount of ethanol and Nafion solution homogeneously to form slurry, and then a few drops was dripped on the GCE followed by dried in air. The loading mass of photocatalyst was about 0.4 mg cm⁻². The applied potential on work electrode was 0.4 V (vs. Ag/AgCl). The 300 W Xe lamp also with a 420 nm cut-off filter cast the light on the surface of the GCE from the front side with the integrated light intensity of 340 mW/cm².



Scheme S1. The possible processes during the synthesis of BD-C₃N₄ by thermal-initiation polymerization of urea and m-Trihydroxybenzene.

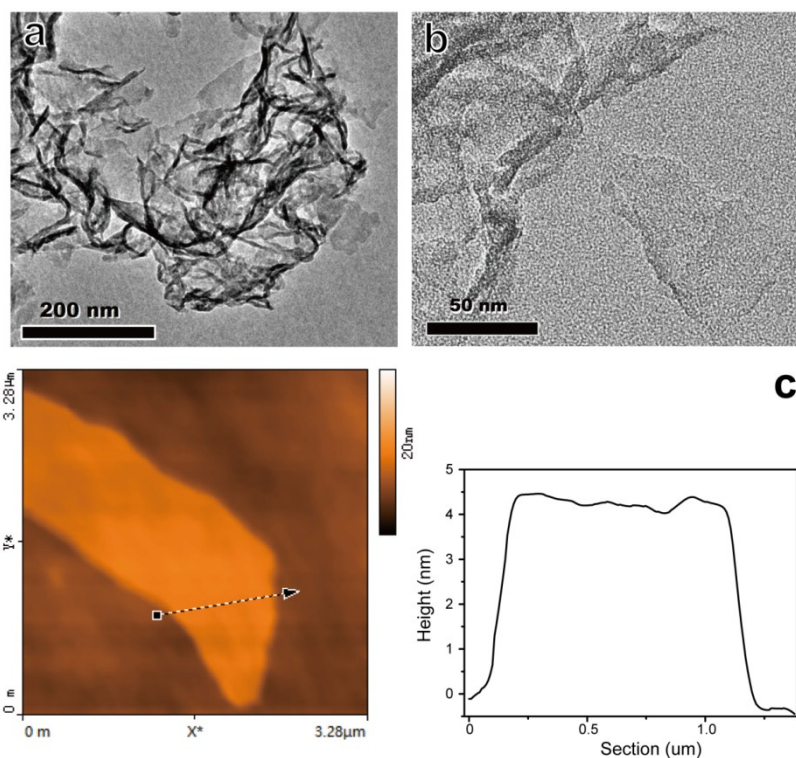


Figure S1. TEM images (a,b), AFM image and height profile (c) of pure g-C₃N₄.

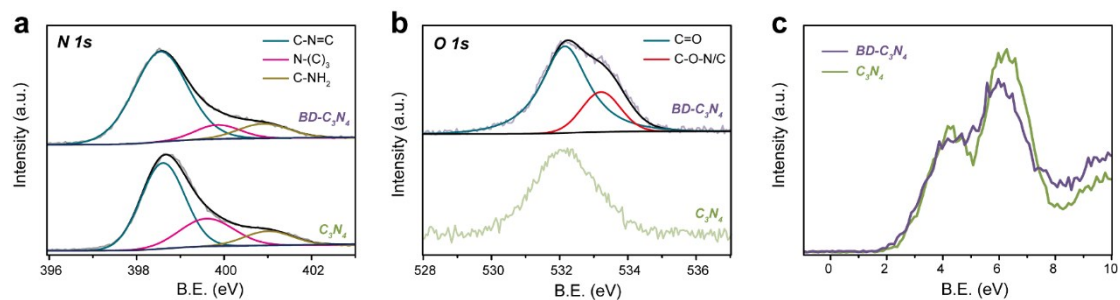


Figure S2. The N 1s (a) and O 1s (b) XPS profiles of BD-C₃N₄ (top) and g-C₃N₄ (bottom), (c) valence band spectra of BD-C₃N₄ and g-C₃N₄.

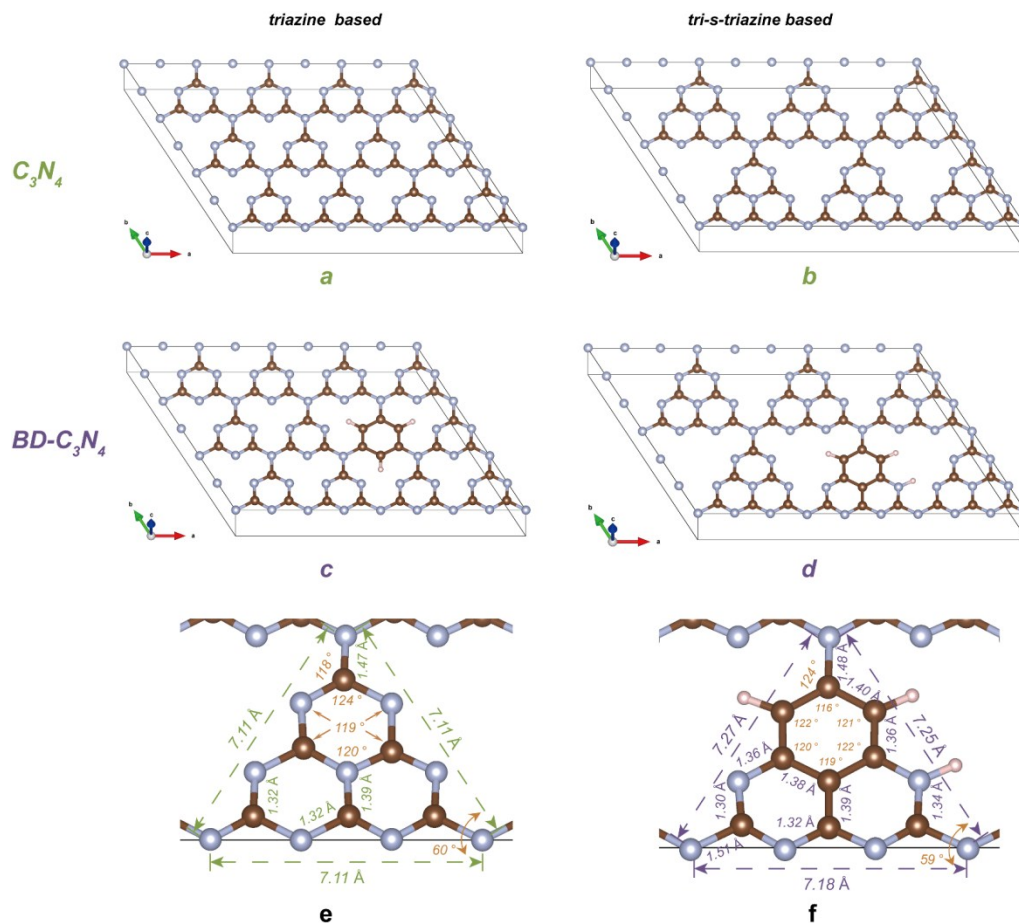


Figure S3. The triazine (a, b) and tri-s-triazine based (c, d) plane based structure of g-C₃N₄ (a, b) and BD-C₃N₄ (c, d). The N, C, and H atoms were represented in brown, white and pink. The amplification of common (e) and benzene ring-containing (f) tri-s-triazine units.

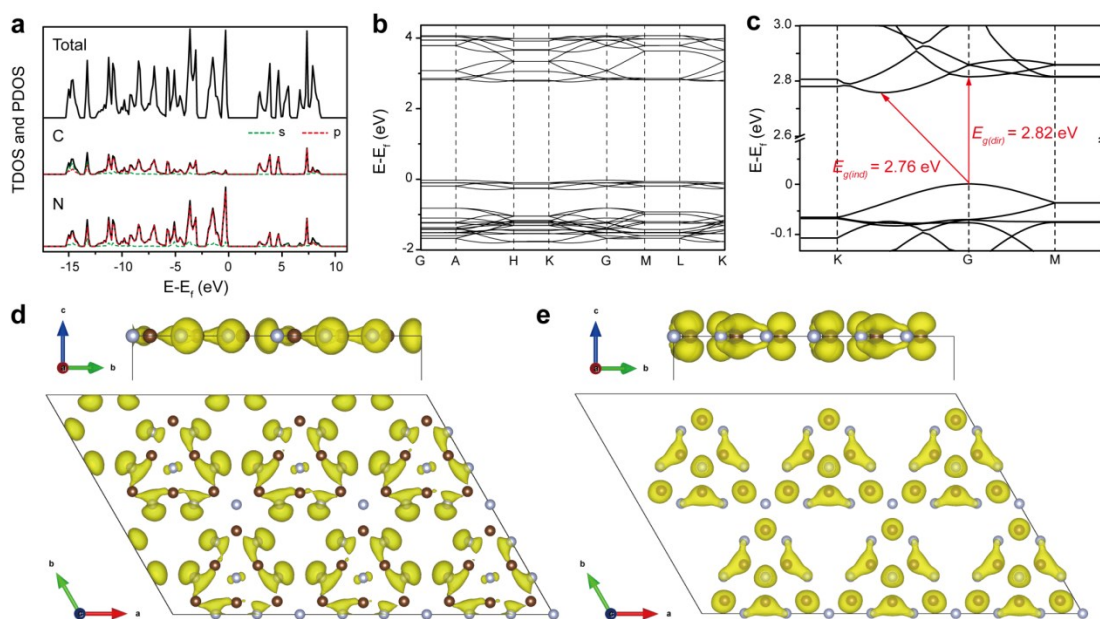
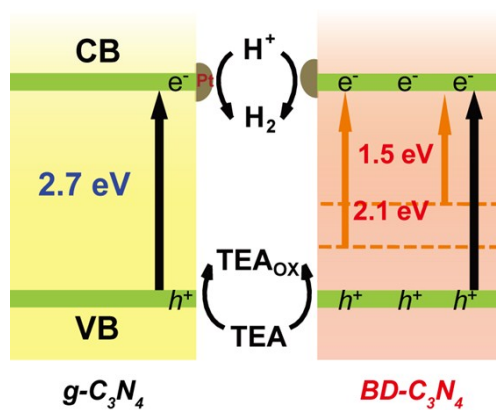


Figure S4. TDOS and PDOS profiles (a), band structure (b, c) and band decomposed charge-density distribution at valence-band maximum (d, side-view image in the top and top-view image in the bottom) and conduction-band minimum (e) of $g\text{-C}_3\text{N}_4$. N and C atoms were represented in white and brown respectively.



Scheme S2. The diagrammatic comparison of band structures of $g\text{-C}_3\text{N}_4$ and $BD\text{-C}_3\text{N}_4$

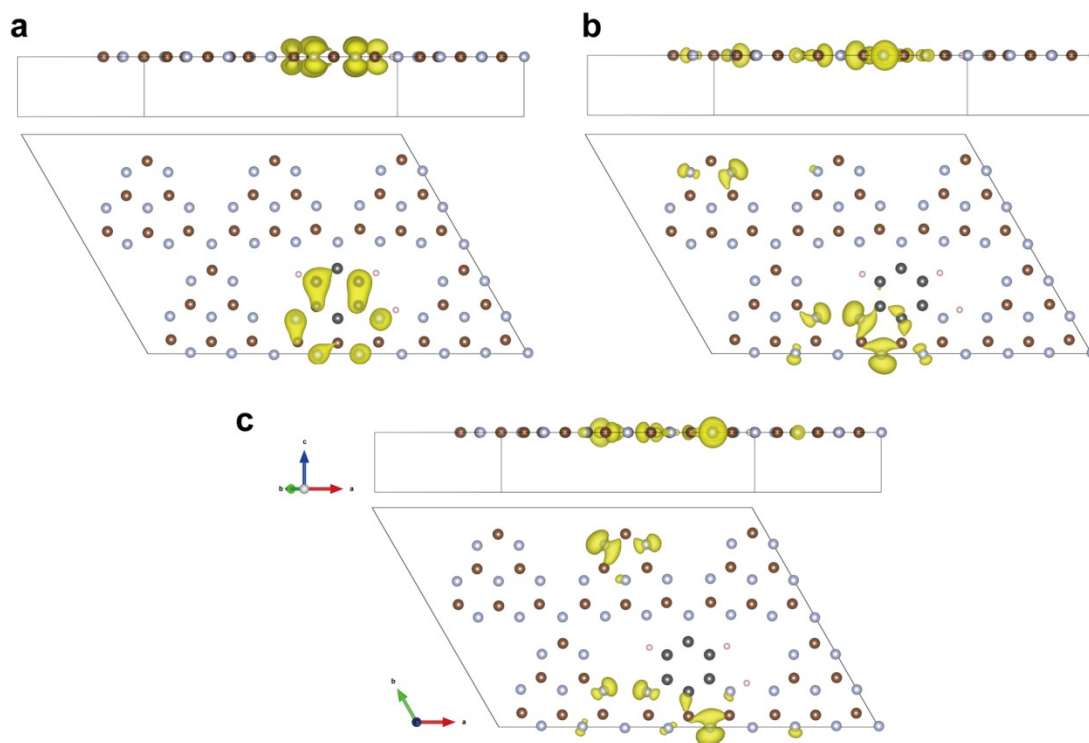


Figure S5. The band decomposed charge-density distribution of *band A* (a), *B* (b), and *C* (c) in the band structure of g-C₃N₄ in Figure 3d (side-view image in the top and top-view image in the bottom). N, triazine C, aromatic C, and H atoms were represented in brown, white and pink respectively.

Table S1. The radiative fluorescence lifetimes and their relative percentages of photoexcited charge carriers in of g-C₃N₄ and BD-C₃N₄.

τ (ns) ^[a]	g-C ₃ N ₄		τ (ns)	BD-C ₃ N ₄	
	<i>A</i> ^[a]	τ_A (ns) ^[a]		<i>A</i>	τ_A (ns)
2.34	2334.45		2.59	52.74	
7.60	1131.42	14.85	11.41	24.62	22.42
30.30	286.57		58.58	2.74	

[a] τ : lifetime, *A*: effective intensity, τ_A : average lifetime.

Time-resolved fluorescence decay spectra of g-C₃N₄ and BD-C₃N₄ were monitored at 460 and 536 nm respectively by time-correlated single-photon counting under the incident light of 370 nm. The decay curves were fitted based on the equation: $y = y_0 + A_1 \exp(-t/\tau_1) + A_2 \exp(-t/\tau_2) + A_3 \exp(-t/\tau_3)$. The average lifetime was calculated by using the equation: $\tau_A = (A_1 \tau_1^2 + A_2 \tau_2^2 + A_3 \tau_3^2) / (A_1 \tau_1 + A_2 \tau_2 + A_3 \tau_3)$.

Table S2. The comparison in hydrogen evolution efficiency between BD-C₃N₄ and other reported doping modified g-C₃N₄ photocatalysts.

<i>Doped unit</i>	<i>Method</i>	<i>Raw materials</i>	<i>Hydrogen evolution rate (mmol h⁻¹ g⁻¹)</i>	<i>Ref</i>
I	Copolymerization	Dicyandiamide + ammonium iodine	0.76	2
O	Copolymerization	Melamine + hydrogen peroxide	1.204	3
O	Hydrothermal treatment	g-C ₃ N ₄ + H ₂ O ₂	0.375	4
S	Copolymerization	Thiourea	1.36	5
S	Annealing	g-C ₃ N ₄ under H ₂ S (air)	< 0.4	6
P	Copolymerization	Guanidiniumhydrochloride + Hexachlorocyclotriphosphazene	0.506	7
P	Copolymerization	melamine + phosphorous acid	0.67	8
Zn	Solvent-thermal treatment	g-C ₃ N ₄ + ZnCl ₂	0.297	9
Defect	Annealing	Dicyandiamide under H ₂ (air)	< 0.1	10
Hydrogenated Defect	Annealing	g-C ₃ N ₄ under H ₂ (air)	0.96	11
Quinazoline	Copolymerization	Dicyandiamide + aminobenzonitrile	2.29	12
Benzene ring	Copolymerization	Urea + <i>m</i> -Trihydroxybenzene	3.167	This work

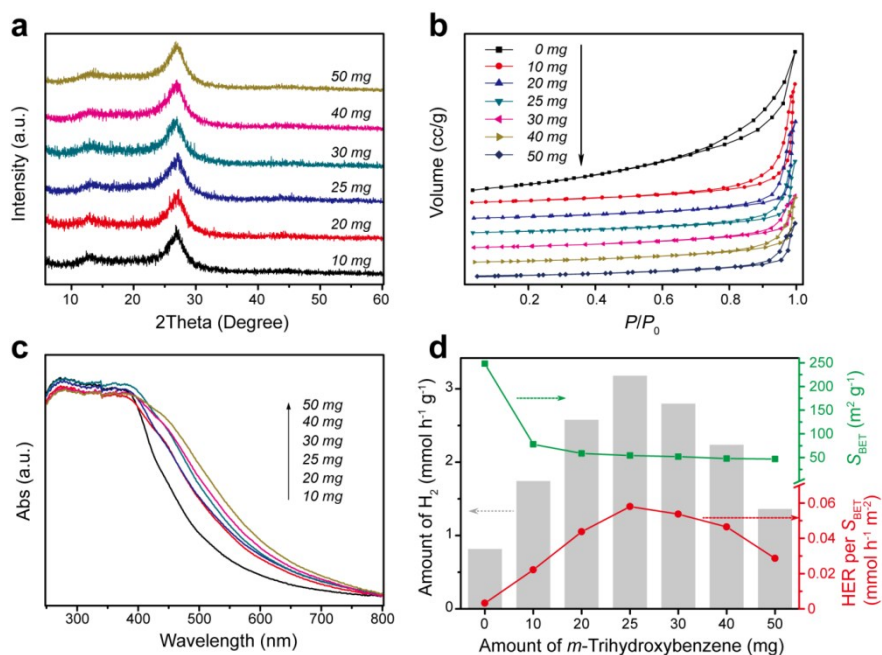


Figure S6. The XRD patterns (a), N_2 adsorption-desorption isotherm curves (b), UV-Vis absorption spectra (c), and (d) H_2 evolution rates (histogram, left axis), BET specific areas (green dot and line, right-top axis), H_2 evolution rates versus specific areas (green dot and line, right-bottom axis) of $BD-C_3N_4$ with different amounts of *m*-Trihydroxybenzene in the polymerization (etching time: 1.5 h; polymerization temperature: 550 °C).

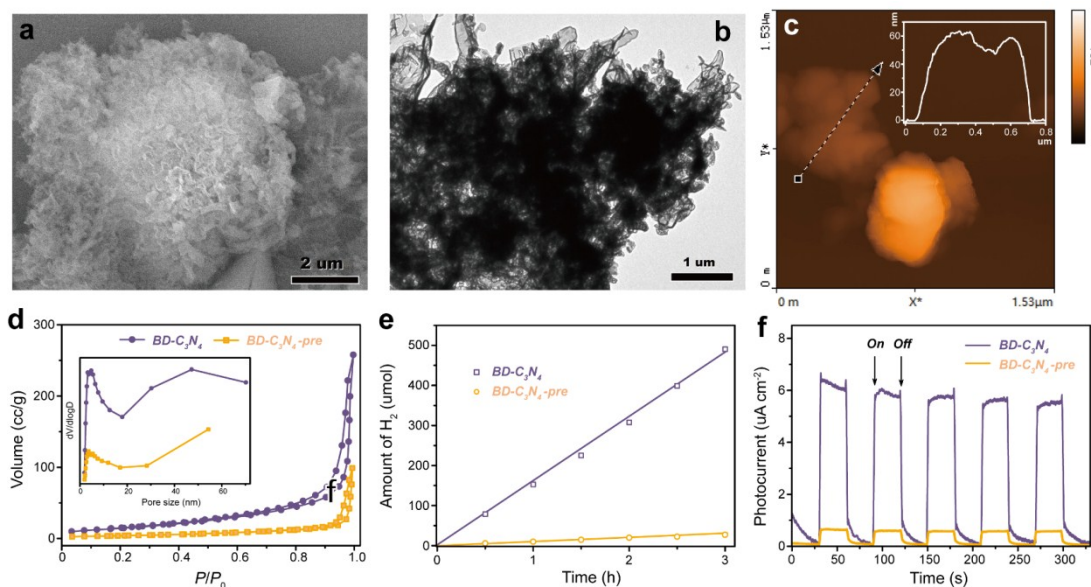


Figure S7. SEM (a), TEM (b), AFM image and height profile (c) of $BD-C_3N_4$ precursor (without heat-etching). (d) N_2 adsorption-desorption isotherm curves (inset showed pore size distributions), (e) photocatalytic H_2 evolution efficiencies, (f) photocurrent curves versus time of $BD-C_3N_4$ and the precursor.

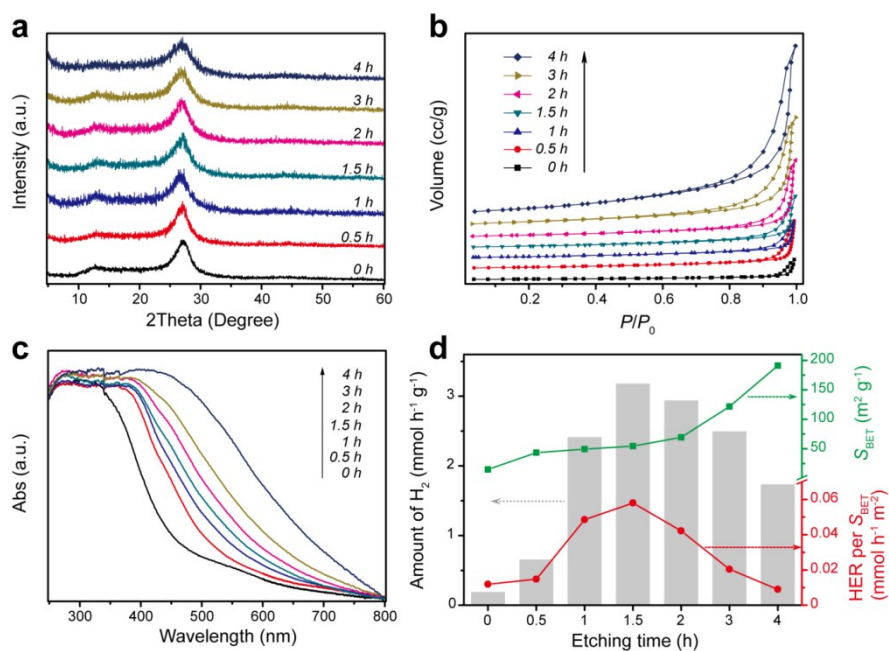


Figure S8. The XRD patterns (a), N₂ adsorption-desorption isotherm curves (b), UV-Vis absorption spectra (c), and (d) H₂ evolution rates (histogram, left axis), BET specific areas (green dot and line, right-top axis), H₂ evolution rates versus specific areas (green dot and line, right-bottom axis) of BD-C₃N₄ with different etching times (amount of of *m*-Trihydroxybenzene: 25 mg; polymerization temperature: 550 °C).

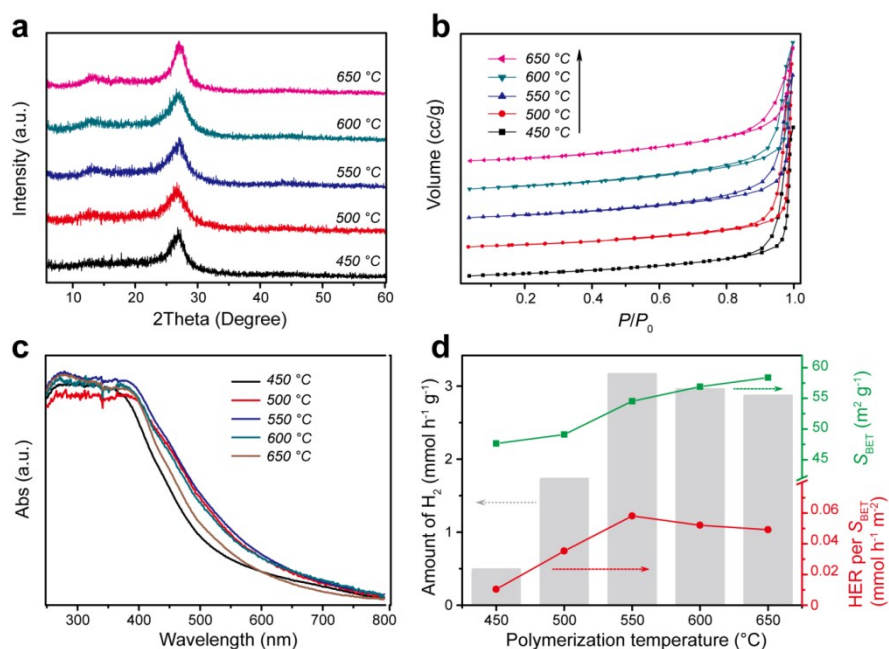
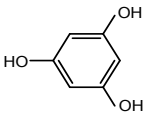
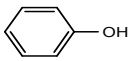
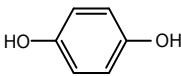
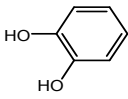
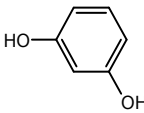
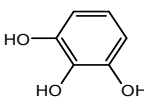
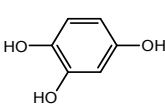
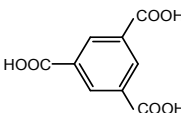
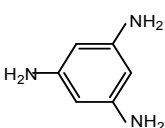
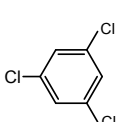


Figure S9. The XRD patterns (a), N₂ adsorption-desorption isotherm curves (b), UV-Vis absorption spectra (c), and (d) H₂ evolution rates (histogram, left axis), BET specific areas (green dot and line, right-top axis), H₂ evolution rates versus specific areas (green dot and line, right-bottom axis) of BD-C₃N₄ under different polymerization temperatures (amount of of *m*-Trihydroxybenzene: 30 mg for 450 °C, 10 mg for 650 °C, 25 mg for others; etching temperature and time: 550 °C and 1.5 h).

Table S3. The photocatalytic hydrogen evolution activity of some other modified g-C₃N₄ by copolymerization of urea with different substituted benzene co- monomer (including location, number and type).

<i>Doped unit</i>	<i>Doped amount</i> ^[a] (mg : 10 g urea)	<i>Specific surface area</i> (<i>S</i> _{BET} m ² g ⁻¹)	<i>Amount of H₂</i> (mmol h ⁻¹ g ⁻¹)	<i>HER per S_{BET}</i> (mmol h ⁻¹ m ⁻²)
	30	54.54	3.167	0.0581
	20	139.35	1.103	0.0079
	20	73.12	0.265	0.0036
	20	63.50	0.900	0.0142
	20	66.77	0.550	0.0082
	30	68.73	0.973	0.0142
	30	49.87	0.537	0.0108
	30	44.22	0.972	0.0220
	30	53.44	0.834	0.0156
	30	52.96	0.855	0.0161

[a] The doped amount used for different substituted benzene co-monomers was specially optimized to achieve the highest performance. The doped amounts exhibited in this table were their optimum doped amounts.

References

1. J. Heyd, G. E. Scuseria and M. Ernzerhof, *J. Phy. Chem.*, 2003, **118**, 8207-8215.
2. G. Zhang, M. Zhang, X. Ye, X. Qiu, S. Lin and X. Wang, *Adv. Mater.*, 2014, **26**, 805-809.
3. Z.-F. Huang, J. Song, L. Pan, Z. Wang, X. Zhang, J.-J. Zou, W. Mi, X. Zhang and L. Wang, *Nano Energy*, 2015, **12**, 646-656.
4. J. Li, B. Shen, Z. Hong, B. Lin, B. Gao and Y. Chen, *Chem. Commun.*, 2012, **48**, 12017-12019.
5. J. Hong, X. Xia, Y. Wang and R. Xu, *J. Mater. Chem.*, 2012, **22**, 15006-15012.
6. G. Liu, P. Niu, C. Sun, S. C. Smith, Z. Chen, G. Q. Lu and H.-M. Cheng, *J. Am. Chem. Soc.*, 2010, **132**, 11642-11648.
7. Y. Zhou, L. Zhang, j. Liu, X. Fan and J. Shi, *J. Mater. Chem. A*, 2015, **3**, 3862-3867.
8. S. Guo, Z. Deng, M. Li, B. Jiang, C. Tian, Q. Pan and H. Fu, *Angew. Chem. Int. Edit.*, 2016, **55**, 1830-1834.
9. Y. Bing, L. Qiuye, I. Hideo, K. Tetsuya and Y. Jinhua, *Sci. Tech. Adv. Mater.*, 2011, **12**, 034401.
10. Q. Tay, P. Kanhere, C. F. Ng, S. Chen, S. Chakraborty, A. C. H. Huan, T. C. Sum, R. Ahuja and Z. Chen, *Chem. Mater.*, 2015, **27**, 4930-4933.
11. X. Li, G. Hartley, A. J. Ward, P. A. Young, A. F. Masters and T. Maschmeyer, *J. Phy. Chem. C*, 2015, **119**, 14938-14946.
12. J. Zhang, G. Zhang, X. Chen, S. Lin, L. Möhlmann, G. Dołęga, G. Lipner, M. Antonietti, S. Blechert and X. Wang, *Angew. Chem.*, 2012, **124**, 3237-3241.